JOURNAL OF CATALYSIS 137, 473–486 (1992)

The Transient Species Formed over $Ru-RuO_x/TiO_2$ Catalyst in the CO and CO + H_2 Interaction: FTIR Spectroscopic Study

N. M. GUPTA,* V. S. KAMBLE,* R. M. IYER,* K. RAVINDRANATHAN THAMPI,† AND M. GRÄTZEL†

*Chemistry Division, Bhabha Atomic Research Centre, Trombay, Bombay 400085, India; and †Institute of Physical Chemistry, Swiss Federal Institute of Technology, Lausanne, CH 1015, Switzerland

Received November 14, 1991; revised April 23, 1992

At least six C–O stretch vibrational bands at around 2142, 2132, 2085, 2050, 1995, and 1950 cm^{-1} were detected in the room temperature adsorption of both CO and CO + H_2 over titania-supported partially reduced ruthenium. These bands were identifiable with the reported multicarbonyl and the linear-bonded monocarbonyl species and indicate that the different oxidation states of ruthenium serve as independent CO chemisorption sites which may coexist on a real catalyst surface at a particular temperature. The effect of exposure temperature and that of the postexposure thermal annealing on CO vibrational bands suggest that the multicarbonyl species transform progressively to monocarbonyl forms which are in turn identified as precursors to the methylene groups in the presence of hydrogen. Though the presence of hydrogen had no apparent effect on the shape and the frequency of different C–O stretch bands, it promoted the above transformations to a considerable extent. In addition to the C–O stretch bands, CO + H_2 interaction at temperatures above 400 K gave rise to hydrocarbon structures consisting of a chain of methylene groups. When in nascent form, these hydrocarbons were very reactive toward hydrogen but on thermal treatment in the absence of hydrogen they were converted to an inactive form. The presence of these hydrocarbon chains blocked binding sites responsible for $\nu_{CO} = 2050\ cm^{-1}$ monocarbonyl species, resulting in the continuous decrease in their concentration and hence in the red shift of corresponding bands with increase in exposure temperature. The promotional effect of oxidized ruthenium and the role of oxygenated surface complexes in CO methanation are discussed in light of the present results.

INTRODUCTION

The activity and selectivity of various group VIII metals for hydrogenation of carbon oxides depend on the composition, dispersion, and oxidation state of the metal in addition to the nature of the support and the extent of metal–support interaction [recent reviews, (*1–6*)]. The mode in which reacting molecules are chemisorbed over the catalyst surface is also found to depend on the nature of the metal used. It is, however, not clearly understood how the mode of CO adsorption influences the activity or selectivity of a metal. Various other questions pertaining to CO hydrogenation also remain unanswered. For example, Hoffman and Robbins (*7*) have shown that though the presence of coadsorbed hydrogen increased the dissociation rate of CO by more than two orders of magnitude, it did not cause any significant changes in the IR bands due to adsorbed CO. The role played by hydrogen in the CO hydrogenation reaction, however, still remains unresolved. A further question concerns the observed enhancement of catalytic activity when a part of the catalyst metal is present in the oxide form (*8–13*).

Fewer IR studies have been reported on CO adsorption using Ru/TiO_2 as a catalyst (*13–15*) compared to those using Ru/SiO_2 (*16–29*), Ru/Al_2O_3 (*17, 19, 30–33*), and Ru/zeolite (*34*) catalysts. In the present study, we have attempted to focus on the nature of the transient species formed over the RuO_x/TiO_2 ($x \leq 2$) catalyst during the

0021-9517/92 $5.00

exposure to CO or CO + H_2. The catalyst under study was found to exhibit high CO and CO_2 methanation activity compared to a completely reduced Ru/TiO_2 sample (*8*). Using this catalyst, the onset of detectable methane formation from CO_2 was observed at around 325 K, whereas the corresponding temperature for CO methanation was 400 K (*37*). To understand the species responsible for this kinetic behavior and to answer some of the questions raised above, we have recorded IR spectra of $Ru–RuO_x/TiO_2$ on exposure to CO and CO + H_2 at various sample temperatures in the range 300–500 K, and the time- and temperature-dependent stability of various vibrational bands was evaluated. The FTIR spectrophotometer employed in this study was coupled to an external sample compartment housing a gas cell which enabled us to periodically analyze effluents generated in the above reactions.

EXPERIMENTAL

Catalyst

The $Ru–RuO_x/TiO_2$ catalyst was prepared using a method described earlier (*8*). It had a surface area of about 55 $m^2 g^{-1}$ and consisted of 3.8 wt% ruthenium. The metal dispersion and the distribution of Ru in different oxidation states at the catalyst surface as evaluated by transmission electron microscopy and H_2 chemisorption measurements have been reported elsewhere in detail (*14, 35, 36*). A typical 3.8% $Ru–RuO_x/TiO_2$ catalyst exhibited a metal dispersion of better than 82% (*35*). About 25% ruthenium existed in the zero oxidation state and the rest in oxidation states corresponding to $x < 2$ (*8, 36*). Electron microscopy revealed that the ruthenium particle size ranged between 10 and 30 Å. For the sake of convenience, the catalyst is henceforth referred to as Ru/TiO_2 in the text.

IR Spectroscopy

The IR studies were performed in transmission mode using a stainless steel cell consisting of CaF_2 windows fixed on water-cooled flanges. The path length between two windows was about 6 cm. A self-supporting catalyst wafer 2.5 cm in diameter and weighing about 70 mg was placed in the path of the IR beam and could be heated at controlled temperatures up to 625 K. The sample temperature was monitored using a fine nickel chrome–nickel thermocouple junction fixed directly at the edge of the catalyst wafer. Because of the large dimension of the catalyst pellet a difference of about 5–10 K in the temperature at the edge and at the middle portion of the pellet was observed. The cell was coupled to a vacuum system ($\sim 10^{-4}$ Torr)/gas manifold and its pressure was regularly monitored using a penning gauge or a Druck digital pressure transducer.

A Mattson (USA) FTIR spectrophotometer (Model Cygnus-100) equipped with a DTGS detector and a KBr beam splitter was employed to record IR spectra. For each spectrum 60 to 300 scans were added at 4 cm^{-1} resolution as required. Recording of data thus covered about 2 to 11 min of reaction time.

Methods

Before exposure to an adsorbate, all the samples were pretreated in hydrogen for about 2 h at 460 K and then for about 2 h under vacuum at 525 K. A rather low pretreatment temperature was chosen to preserve the oxidation state of ruthenium. It was, however, not possible to precisely evaluate any modifications in the ruthenium oxidation states occurring as a result of *in situ* pretreatments given to a sample or when a particular catalyst wafer was employed repeatedly for a series of experiments. The IR spectrum of the wafer was recorded to serve as a reference. The sample was then exposed at different temperatures to CO or CO + H_2 (1 : 3) either under flow (5–10 ml min^{-1}) or under static mode. Both the sample and the background spectra were normally recorded at the exposure temperature to minimize the temperature effects. To compensate for the IR bands due to gaseous

adsorbates in the cell, corresponding spectra were also recorded using an identical wafer prepared form the metal-free titania. Difference spectra were obtained initially in the absorbance mode and were then plotted as transmittance. The time- and temperature-dependent transformations in the surface species were monitored after pumping out gaseous adsorbates from the cell. Fourier self-deconvolution spectra were also recorded to resolve various overlapping C–O stretch bands in the 1850–2200 cm^{-1} region. For this purpose, various combinations of parameters, such as full width at half maximum (w = 10 to 60 cm^{-1}) and amplification factor (k = 1 to 2), were tried. The best results were obtained for values of w in the 40 to 50 cm^{-1} range and for a k value of around 1.4. Whereas various bands merged together for higher w values, the larger values of k resulted in the amplification of noise signals.

Carbon monoxide of 99.5% purity from Airco (USA) was used after passing through a solidified carbon dioxide (195 K) trap to remove any carbonyl or moisture impurities. H_2 and He gases were passed through oxisorb and molecular sieves traps for further purification.

RESULTS

CO + H_2 Exposure under Continuous Flow

Various overlapping bands in the 2150–1900-cm^{-1} region were observed on Ru/TiO_2 after exposure to CO + H_2 (1 : 3) flow at ambient temperature. In addition, bands were also observed due to CO_2 (2358, 2340 cm^{-1}), gaseous CO (2172.5, 2116 cm^{-1}), and small bands at 1620 and 1378 cm^{-1} due to oxygenated species. The shape and frequency of IR bands were found to be independent of the duration of CO + H_2 exposure. Spectrum a in Fig. 1, for example, was recorded after about 30 min of CO + H_2 flow over the catalyst surface. Various changes were, however, observed on raising the sample temperature. First, a new pair of bands with maxima at around

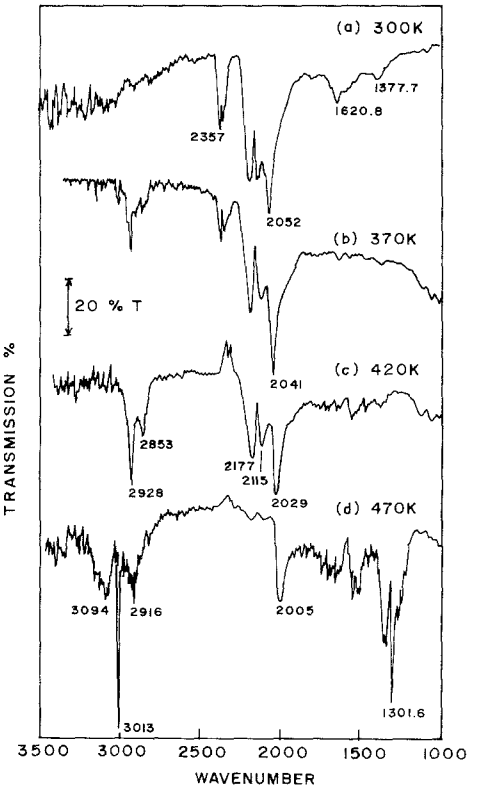

FIG. 1. Infrared spectra of partially reduced Ru/TiO_2 after 30 min exposure to CO + H_2 (1 : 3) flow at various sample temperatures.

2928 and 2853 cm^{-1} was detected at sample temperatures in the range 350–420 K, the intensity of which increased with the exposure temperature. A weak shoulder peak was also discernable at about 2960 cm^{-1}. Spectra b and c of Fig. 1 illustrate these bands in the data observed at two exposure temperatures of 370 and 420 K. However, the intensity of these peaks reduced progressively with further increase in sample temperature and a new sharp peak due to methane appeared at 3013 cm^{-1}. At exposure temperatures greater than 425 K, a set of intense bands due to gaseous CH_4 was observed in lieu of the bands at 2928 and 2853 cm^{-1} (Fig. 1d). Second, the intensity of the CO_2 bands (2358 and 2340 cm^{-1}) was also found to be reduced with the progressive increase in sample temperature (Fig. 1a–1d).

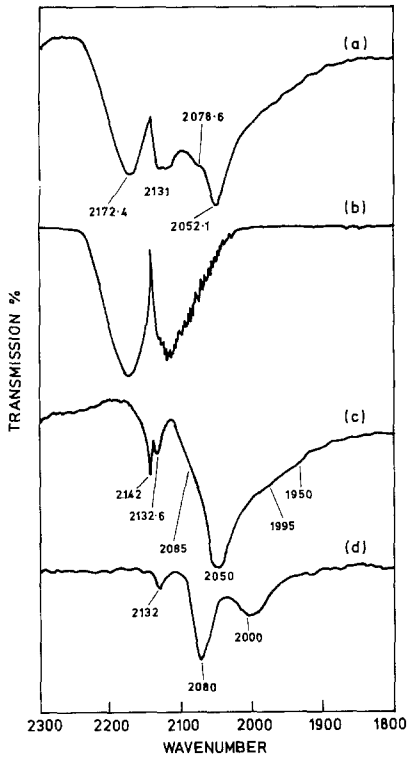

FIG. 2. Vibrational spectra of the C–O stretching region when (a) Ru/TiO_2 and (b) TiO_2 were exposed to CO + H_2 (1 : 3) flow for 30 min. (c) Spectrum obtained on subtraction of b from a; (d) IR spectrum of Ru/TiO_2 after 20 min evacuation following 1 h CO + H_2 flow at 300 K.

Temperature Effect on C–O Stretch Bands

Increase in the sample temperature also had considerable effect on IR bands in the C–O stretch region. Figure 2a shows the C–O stretch region spectrum recorded after 30 min CO + H_2 flow over Ru/TiO_2 at 300 K. Spectrum b in this figure was obtained for a metal-free TiO_2 wafer recorded under identical conditions of CO + H_2 flow at 300 K. Curve c, obtained on computer subtraction of spectrum b from spectrum a, thus presents IR bands due to species deposited at Ru sites or at Ru/TiO_2 interfaces. A Fourier self-deconvolution revealed, in addition to two bands at 2142 and 2132 cm^{-1} seen in Fig. 2c, the broad 2100–1900 cm^{-1} region C–O stretch band comprising four distinct bands with maxima around 2092, 2048, 1996, and 1954 cm^{-1}. Figure 3 presents such a deconvolution spectrum. The presence of various bands mentioned above was further confirmed in the parallel experiments performed using isotopically labeled ^{13}CO as an adsorbate (*37*).

Pumping of gases from the IR cell resulted in the progressive removal of some of the bands in Fig. 2c. Spectrum d in Fig. 2, consisting of bands at 2132, 2080, and 1995 cm^{-1}, was recorded after 20 min of sample evacuation. Prolonged evacuation had no further effect on the IR bands in the spectrum of Fig. 2d, but raising the sample temperature led to their removal.

The increase in exposure temperature resulted in the progressive removal of high frequency C–O stretch bands and also in the shift of the 2050-cm^{-1} band to a lower frequency. Figure 4 exhibits IR spectra in C–O stretch region recorded after 20–30 min of CO + H_2 flow over Ru/TiO_2 at various temperatures in the range of 300 to 475 K. A single catalyst wafer was used for these experiments and was given a hydrogen and a vacuum pretreatment each time, as described under Methods, prior to initiating CO + H_2 flow at the desired temperature. It may also be mentioned that both the sample

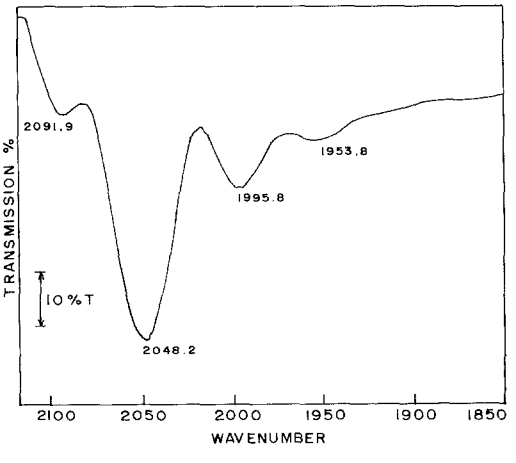

FIG. 3. Deconvolution and expansion of Fig. 2c (deconvolution parameters: w = 50 cm^{-1}, k = 1.4, f = 0.4, and Bessel function).

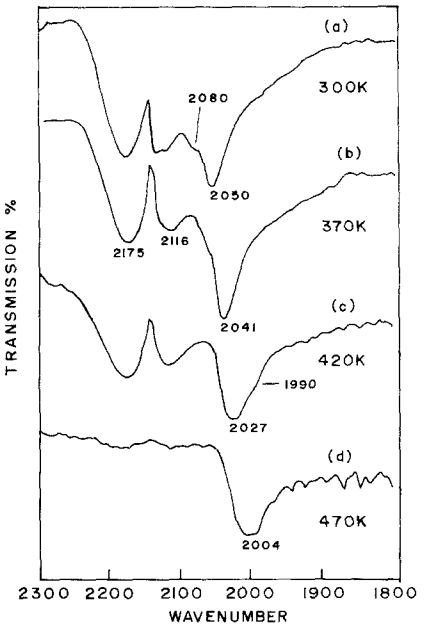

FIG. 4. Vibrational spectra of the C–O stretching region obtained after exposing the Ru/TiO_2 catalyst at various temperatures to CO + H_2 (1 : 3) flow. Spectra recorded 20–30 min after commencement of flow.

and the background spectra were recorded at the exposure temperature in a particular experiment and the gas pressure in the cell remained constant at 757 ± 0.5 Torr throughout the experiments reported in Fig. 4. Figure 4 shows that the bands at 2132 and 2085–2090 cm^{-1} disappear completely at a sample temperature of 420 K. Also, the most intense band at 2050 cm^{-1} shifted to 2041, 2027, and 2004 cm^{-1} for the exposure temperatures of 370, 420, and 470 K, respectively. Another important feature of Fig. 4 is reflected in the emergence of a distinct band at around 1990 cm^{-1}, the intensity of which increased considerably with the increase in the gas exposure temperature (Figs. 4c and 4d).

After recording the data shown in Fig. 4 when the sample was recooled to lower temperatures, while maintaining a constant flow and pressure of CO + H_2, the ν_{CO} was not restored to its original values. Thus the frequency of the 2004-cm^{-1} band in Fig. 4 either remained unchanged or was further reduced by a few wavenumbers when the sample was cooled back to ambient temperature. This behavior differs from that reported by Hoffmann and Robbins using a Ru single crystal (*7*). It is also pertinent to mention here that in addition to intense bands at 2928 and 2853 cm^{-1}, a broad absorbance band was developed in the 2600- to 3500-cm^{-1} region when the sample was cooled to ambient temperature under CO + H_2 flow subsequent to heating up to 470 K.

Effect of Exposure Time

When the IR spectra were recorded as a function of time after switching CO + H_2 flow at a particular temperature, the peak positions were found to remain by and large unchanged except for the experiments performed at 470 K, when the main peak appearing initially at around 2010 cm^{-1} was removed progressively with time, whereas the intensity of another peak at 1990 cm^{-1} increased simultaneously. Spectra a–d in Fig. 5 present the time evolution of CO

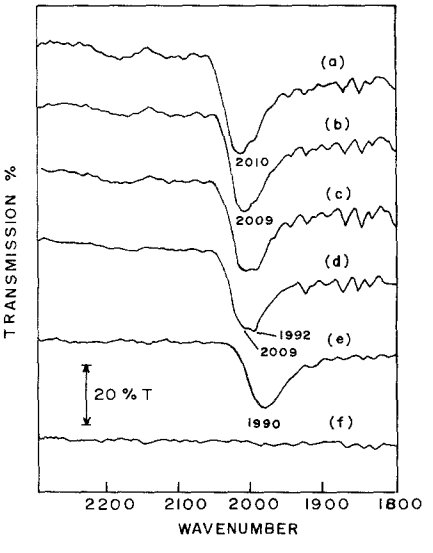

FIG. 5. Infrared spectra of adsorbed CO as a function of exposure time when a Ru/TiO_2 catalyst was exposed to CO + H_2 (1 : 3) flow at 470 K for (a) 0.5 min, (b) 5 min, (c) 15 min, and (d) 30 min. Spectra e and f were obtained after evacuation of d at 470 K for 5 and 20 min, respectively.

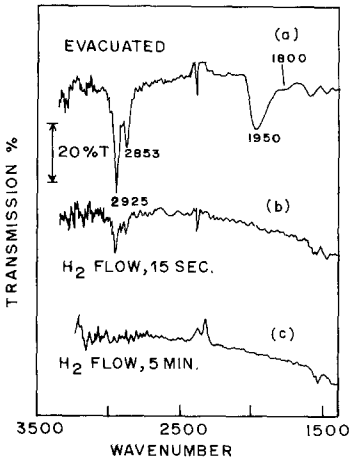

FIG. 6. Effect of H_2 exposure (420 K) on the C–H and C–O stretch bands over Ru/TiO_2 sample exposed to CO + H_2 (1 : 3) flow at 420 K and then evacuated at the same temperature for 30 min.

stretch bands in the exposure of CO + H_2 flow over the Ru/TiO_2 wafer at 470 K. The 2010-cm^{-1} band was removed completely when the IR cell was subsequently evacuated for a few minutes leaving a broad band at about 1990 cm^{-1} (Fig. 5e) with a shoulder peak at around 1950 cm^{-1}. All the IR bands were eventually removed when the cell was evacuated for a longer period while maintaining the sample at 470 K (Fig. 5f).

Stability of 2928- and 2853-cm^{-1} Bands

The IR bands at 2928 and 2853 cm^{-1} (Fig. 1) were found to persist under continuous CO + H_2 flow and were not removed easily on subsequent prolonged evacuation of the sample at the exposure temperature. However, when the sample was brought under hydrogen flow following pumping of residual gases from the cell, the intensity of these bands reduced drastically and the formation of methane was detected in the effluent. The data in Fig. 6 show the effect of hydrogen exposure on C–H stretch bands generated on CO + H_2 exposure for 1 h at 420 K followed by 30 min evacuation (Fig. 6a). Spectra b and c in Fig. 6 show that the species responsible for the 2928- and 2853-cm^{-1} bands were very reactive toward hydrogen and were removed completely within a few minutes of hydrogen flow. The species giving rise to the 1950-cm^{-1} band (Fig. 6a), though stable under vacuum, were also quickly removed on subsequent hydrogen exposure.

To further explore the nature of species giving rise to the above two bands, a catalyst wafer exposed to CO + H_2 at 420 K for 1 h was cooled to ambient temperature. This sample was wetted with a small amount of carbon tetrachloride which was then decanted over a KBr pellet. The IR spectrum of this pellet recorded after evaporation of the solvent showed two intense bands at about 2918 and 2850 cm^{-1}, as is shown in spectrum a of Fig. 7. Spectrum b of this figure displays corresponding data for a KBr pellet soaked similarly in the pure solvent. This experiment thus suggests that a hydrocarbon species consisting of a long chain of

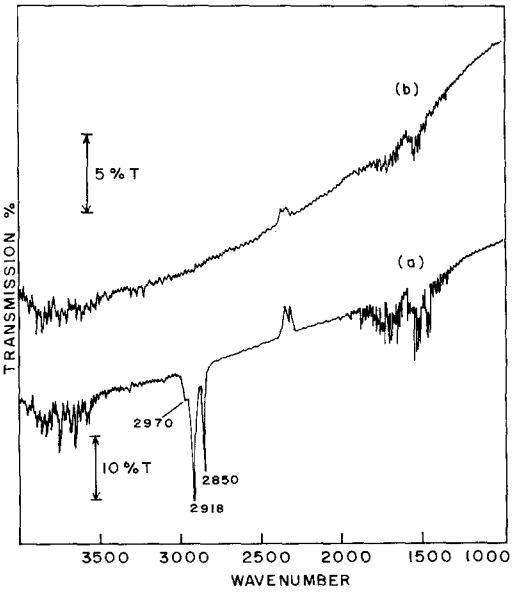

FIG. 7. (a) IR spectrum of KBr pellet impregnated with CCl_4 extract of a deposit formed over Ru/TiO_2 during 1 h exposure to CO + H_2 (1 : 3) at 420 K followed by cooling to room temperature. (b) IR spectrum of KBr pellet treated similarly with CCl_4 which was contacted with unreacted Ru/TiO_2. For both a and b, the solvent was evaporated out after impregnation over KBr pellet and the spectra were recorded with the blank KBr pellet as a reference.

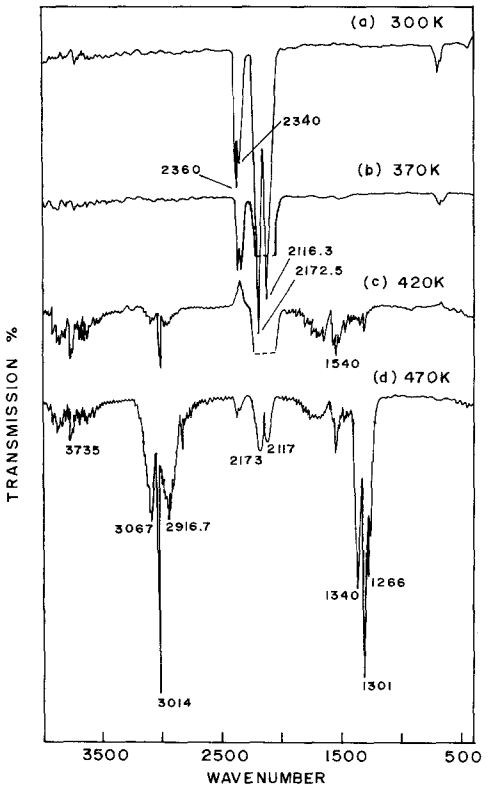

FIG. 8. IR analysis of effluents when a Ru/TiO_2 sample was subjected to CO + H_2 (1 : 3) flow at different temperatures.

($-CH_2$) groups, which, though reactive to hydrogen in the nascent form, eventually converts to a stable form, is produced in the interaction of CO + H_2 at a particular temperature. The referee has drawn our attention to the possibility that the length of the hydrocarbon chain may be evaluated by comparing the intensity of the asymmetric terminal methyl stretch (2970 cm^{-1}) with that of the CH_2 mode (2918 cm^{-1}). This was not attempted in the present work. Detailed investigations are now in progress to establish the identity of these species by collecting a large amount of this sample and its isotopic analogues and studying the spectra over a wider range.

Effluent Analysis

Figure 8 gives IR spectra of reaction products eluted after about 15–20 min on CO + H_2 reaction over the catalyst wafer at a flow rate of 8 ml min^{-1} and at various temperatures. These data reveal formation of CO_2 (2360-, 2340-cm^{-1} bands) during exposure of CO + H_2 at ambient temperature (Fig. 8a). Though the variation in CO_2 yield during continuous CO + H_2 exposure was not investigated over a long period of time in the present study, the independent thermal desorption spectroscopy results have shown that the CO_2 formation resulted from oxygen abstraction from the TiO_2 support (*37*). As seen in Fig. 8, the methane (3014- and 1300-cm^{-1} region bands) formation was detected only at sample temperatures above 400 K (Fig. 8c) whereas almost complete conversion to CH_4 was observed at the sample temperatures of 450 K and above (Fig. 8d). In addition to the IR bands mentioned above and besides vibration–rotation bands due to water vapor in the 3700- and 1500-cm^{-1} regions, a few weak bands at around 2875, 1700, and 1540 cm^{-1} may also be noted in Figs. 8c and 8d. These bands may indicate the formation of small amounts of other CO hydrogenation products besides CH_4 though they remain unidentified at this stage.

CO + H_2 Exposure in Static Mode

Results similar to those described above were observed when Ru/TiO_2 was exposed to CO + H_2 in static mode at various pressures in the range 50–200 Torr (*38*). A distinct feature of these data was the initial appearance of a single band at 2127 cm^{-1} instead of a doublet at 2142 and 2131 cm^{-1} as shown in Fig. 2. The frequency of this band shifted progressively to higher values during prolonged contact with CO + H_2 and attained a value of about 2140 cm^{-1} after about 2 h of exposure.

CO Exposure

Figure 9a shows the IR spectrum of Ru/TiO_2 exposed to 100 Torr of CO for 5 min at ambient temperature. Prolonged exposure to CO resulted in a marginal increase in the intensity of the 2340-cm^{-1} band (Fig. 9b) identifiable with adsorbed CO_2 (*39, 40*).

To compensate for the contribution of gaseous CO present in the cell, a spectrum which showed two C–O stretch bands peaking at about 2172 and 2120 cm^{-1} was recorded after exposing 100 Torr of CO over a metal-free TiO_2 pellet. Spectrum c in Fig. 9 was then obtained by subtracting the CO (100 Torr)/TiO_2 spectrum from spectrum b. As shown earlier, the Fourier self-deconvolution of the difference spectrum in Fig. 9c revealed the presence of distinct peaks at around 2132, 2085, 2045, 1995, and 1930 cm^{-1}.

The C–O stretch bands of Fig. 9c were quite stable and were observed after prolonged evacuation and ambient temperature. Spectrum a of Fig. 10, for example, was recorded after 30 min evacuation of the IR cell following a 100-Torr CO exposure over Ru/TiO_2. However, subsequent hydrogen exposure at ambient temperature resulted in reduced intensity of the bands at 2135 and 2085 cm^{-1} (Fig. 10b). Subsequent rise of the sample temperature to 375 K in the presence of hydrogen led to removal of high-frequency bands and a single band at around 2020 cm^{-1} (Fig. 10c), which was subsequently removed on further elevation of temperature to 420 K (Fig. 10d), was observed.

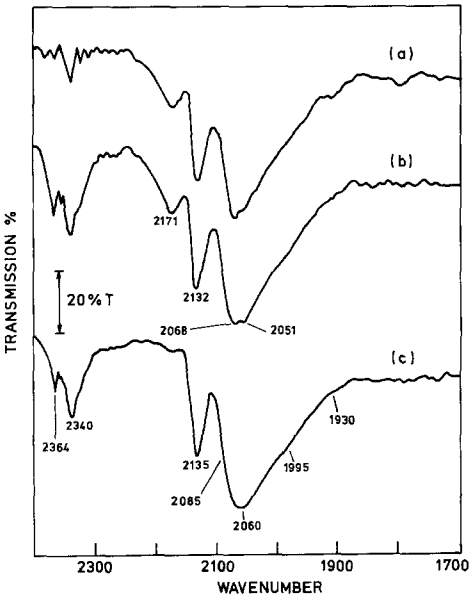

FIG. 9. Infrared spectra of Ru/TiO_2 when 100 Torr of CO was exposed at 300 K for (a) 10 min and (b) 30 min. (c) Difference spectrum obtained on subtraction of TiO_2 – 100 Torr CO spectrum from spectrum b.

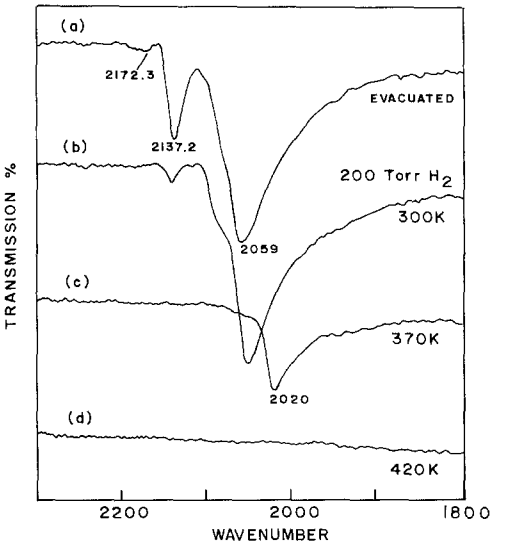

FIG. 10. Spectral changes observed in C–O stretch bands when a Ru/TiO_2 sample exposed at 300 K to 100 Torr of CO was (a) evacuated (30 min) and then (b–d) exposed to 200 Torr of H_2 at different temperatures.

Similar features were observed for CO exposures at higher gas pressures.

Temperature Effect

Higher frequency bands were removed progressively when the CO exposures were made at elevated sample temperatures. Figures 11a and 11b show IR spectra of Ru/TiO_2 samples exposed to 100 Torr of CO at 370 and 470 K, respectively. As shown in spectrum a, CO exposure at 370 K attenuated the IR bands at 2135 and 2085 cm^{-1}. A further rise in the sample temperature to 470 K led to the shift of the main band from 2058 to 2045 cm^{-1} (Fig. 11b). Prolonged contact with CO at 470 K led to further reduction in the frequency of this band to about 2030 cm^{-1} (Figs. 11c and 11d).

Larger frequency shifts were, however, observed when the IR cell was pumped subsequent to CO exposure at 470 K, as shown

in the data of Fig. 12. Thus, the frequency of the main band shifted from 2030 to 1993 cm^{-1} during 1 h of evacuation (Figs. 12b–12d).

CO and CO + H_2 Exposure over Metal-Free TiO_2

To evaluate any contribution of support material in the data obtained in the present study, parallel experiments were performed using metal-free titania, which was subjected to pretreatments similar to those given to Ru/TiO_2 samples. No IR bands except those due to C–O stretch of gaseous CO (at around 2172 and 1220 cm^{-1}) were observed when the CO + H_2 were passed over titania at various temperatures in the range 300–500 K. In the exposure of CO in the static mode, small bands due to adsorbed CO_2 were observed for sample temperatures in the range of 370–500 K.

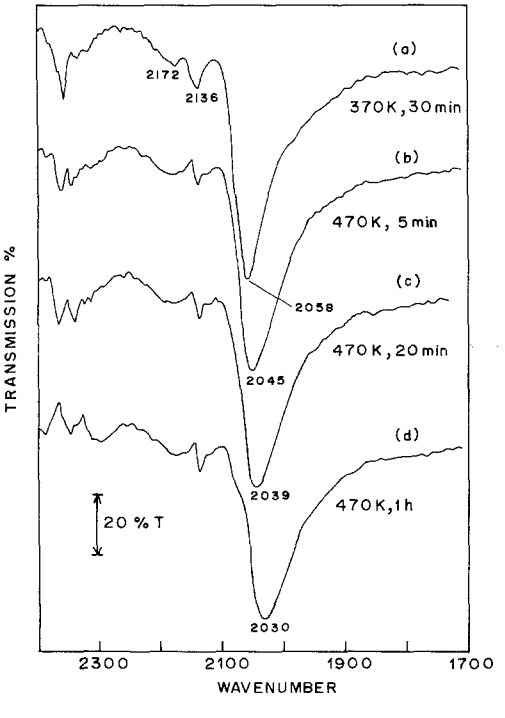

FIG. 11. Effect of exposure temperature and time on the C–O stretch bands when 100 Torr CO was adsorbed over Ru/TiO_2.

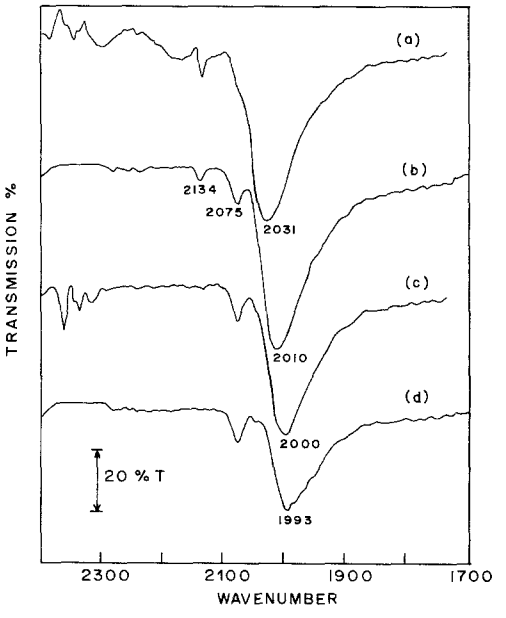

FIG. 12. Effect of evacuation on the C–O stretch bands formed in the adsorption of 100 Torr CO at 470 K over Ru/TiO_2. (a) No evacuation, (b–d) after evacuation at 470 K for 5 min, 20 min, and 1 h, respectively.

DISCUSSION

C–H Stretch Bands

The IR bands in the C–H stretch region have been reported previously by various workers in CO + H_2 reaction using Ru/silica (*19, 29*) and Ru/alumina (*32*) catalysts. These bands are attributed to long chain hydrocarbons comprising CH_2 groups. There have, however, been controversies regarding location, reactivity, and the stability of these groups. Thus, whereas several research groups consider such species to be inactive reaction products deposited at the support surfaces (*29, 32, 41*), in some of the studies (*19*) it is suggested that the methylene or methyl groups are formed at metal sites and serve as precursors to hydrocarbons.

In the present study, we observe two prominent bands at around 2928 and 2853 cm^{-1} when CO + H_2 (1 : 3) were reacted over Ru/TiO_2 (Fig. 1). In addition, a small shoulder at around 2960 cm^{-1} was also discernible. The species formed may be identi-

fied with long chain aliphatic hydrocarbons, since these bands correspond to the asymmetric CH_3 stretch of the end group CH_3 and the methylene groups of a long chain hydrocarbon. A comparison of the data in Figs. 1 and 8 reveals that at a temperature when substantial growth of these bands was detected (Fig. 1), some methane formation was also observed (Fig. 8). But, at the stage of complete conversion of CO to CH_4, no surface methylene groups were detectable (Fig. 1). The data in Fig. 6 show that the surface species were very reactive to hydrogen and the effluent analysis confirmed that the reaction product was methane, though no higher hydrocarbons were detectable, perhaps due to very low yields.

We thus tend to draw the following conclusions from these observations. First, the methylene group chain is formed at Ru sites or at Ru/TiO_2 interfaces and not at the support alone since no such species were formed over metal-free titania. Since the methylene group chains were detectable at a sample temperature of 370 K (Fig. 1b) when no CH_4 was observed in the reaction products (Fig. 8), it is suggested that only at a stage of optimum growth or alternately at an optimum temperature does the hydrocarbon chain become susceptible to bond scisson and hence to the formation of various hydrocarbons on subsequent hydrogenation. The amount of hydrogen available at a reaction site, the chain length, and other reaction conditions, such as the temperature and pressure, may influence the product distribution in a particular experiment. In analogy with the now well-established fact that the nascent carbon formed in CO dissociation over transition metals loses its reactivity with time and converts to a graphite form (*42–44*), it may be postulated that the methylene group chains remain reactive only when in the nascent state. In the absence of hydrogen these species will lead to the polymerized hydrocarbons which are stable under vacuum (Fig. 6a) or are extractable in a solvent such as carbon tetrachloride (Fig. 7). Some of these aspects are now under detailed investigation in our laboratory.

C–O Stretch Region

C–O stretch bands have been the subject of most extensive investigations in CO chemisorption on single crystal or supported noble metals. The frequencies of these bands are found to depend on various factors, such as the nature, dispersion, oxidation state, and crystallographic phase of the exposed metal atom in addition to the nature of support and the surface coverage (*1*). The chemisorption of CO on silica-supported Ru, for example, is known to result in three bands, a low-frequency (LF) band at 2040 ± 10 cm^{-1} and two high-frequency (HF) bands appearing at 2140 ± 10 cm^{-1} (HF_1) and 2080 ± 10 cm^{-1} (HF_2). The low-frequency band is believed to arise from linearly held carbon monoxide over metal crystallites. The logic behind this assignment comes from the fact that a single band at this frequency is widely observed in CO chemisorption over Ru single crystals (*7, 45*). The origin of high-frequency bands has, however, been a matter of controversy. Various models explaining their formation have been proposed and the subject has been reviewed by various authors (*16, 30*). More widely accepted assignments to these bands concern dicarbonyl $M(CO)_2$ or tricarbonyl $M(CO)_3$ type species (*13, 16, 21*). In a recent paper dealing with IR of CO chemisorption over a Ru/TiO_2 catalyst, Robbins (*13*) has shown that the 2085- and 2140-cm^{-1} bands are coupled vibrations due to $Ru(CO)_x$ ($x > 2$) and he assigned them to $(TiO)_2$ $Ru(CO)_3$ surface species. Yokomizo *et al.* (*16*) have shown that the oxidation state of Ru affected these bands considerably. Thus, they observed a set of three bands at 2144 (HF_1), 2082 (HF_2), and 2047 (LF) cm^{-1} when the fully reduced Ru/SiO_2 was exposed to carbon monoxide. On the other hand, the adsorption of CO on partially oxidized Ru/SiO_2 gave rise to corre-

sponding bands at 2136, 2080, and 2032 cm^{-1}. The HF_1/HF_2 intensity ratio was found to be about 0.5. The negative shift in the LF band frequency on CO adsorption over oxidized ruthenium is reported in several other studies also (*20, 21*) and has been attributed to a decrease in the ensemble size of the linearly adsorbed CO on the oxidized catalyst resulting in the decrease in adsorbate–adsorbate interaction (*16, 46, 47*).

In the following we focus on the salient features of the time- and temperature-dependence of C–O stretch bands as observed in the present study.

1. Figures 2c and 3 demonstrate for the first time the simultaneous presence of at least six distinct bands appearing at around 2142, 2132, 2085, 2050, 1995, and 1950 cm^{-1}. These IR bands bear a striking resemblance to the bands reported by Yokomizo *et al.* for Ru/SiO_2 (*16*). Thus, taking the 2142- and 2132-cm^{-1} bands as characteristic of CO chemisorbed over reduced and oxidized Ru sites, respectively, the IR bands in Fig. 2c may be considered to be the sum of bands arising from CO bonded independently to the reduced (Ru^0) and to the oxidized (Ru^{2+}, $Ru^{\delta+}$) metal sites.

Based on the published literature and without considering specific composition of multicarbonyls, possible assignments to IR bands of this study and estimated relative areas under various bands are given in Table 1.

2. In addition to a band at 2050 cm^{-1}, attributed widely to linearly held CO molecules at metal sites, new bands at around 1995 and 1950 cm^{-1} (Fig. 3) are observed in our study. An asymmetric broadening below 2000 cm^{-1} in the C–O stretch region band has been reported in other publications also (*13, 15, 28*), suggesting the possible presence of vibrational bands in this region as confirmed in the present study. As these bands appear during interaction of both the CO and the CO + H_2 and also in view of their proximity to the 2050-cm^{-1} band, we tentatively assign them to the monocarbonyl

TABLE 1

C–O Stretch Bands Observed during Room Temperature Adsorption of CO and CO + H_2 over Partially Reduced Ru/TiO_2 Catalyst

Nomenclature	Frequency (cm^{-1})	Relative intensity		Possible assignment
		CO + H_2 exposure (Fig. 2)	CO exposure (Fig. 10)	
—	2180–2170	—	—	Physisorbed CO
HF_1	2142–2140	0.1	Not observable	$Ru(CO)_n$
HF_1	2134–2132	0.1	0.3	$RuO_x(CO)_n$
HF_2	2090–2080	0.3	0.6	$Ru(CO)_n$ + $RuO_x(CO)_n$
LF_1	2951–2045	1	1	Ru(CO)
LF_1	2000–1985	0.7	0.8	$RuO_x(CO)$
LF_2	1950–1935	0.6	0.5	$RuO_x(CO)$

Note. $0 < x \leq 2$ and $n = 2$ or 3.

form of CO linearly bonded with ruthenium of different oxidation states (Table 1). Ru of 0, 1, and 2 oxidation states is known to coexist in the partially reduced samples.

3. A comparison of the data in Figs. 2 and 9 clearly shows that the species formed during CO + H_2 and CO exposure were quite similar, in both the continuous flow and the static mode experiments. It indicates that the presence of hydrogen does not influence the mode of CO bonding to ruthenium. This is in agreement with the results of IR studies on CO adsorption over Ru (001) single crystals (*7*), over Ru/Al_2O_3 (*30*), and also over a Pd/TiO_2 catalyst (*48*).

4. In contrast to the studies of Yokomizo *et al.* (*16*), who found high frequency bands to be more stable at elevated temperatures or under helium flow, our data reveal that these bands are progressively removed under evacuation and also on thermal annealing (Figs. 2, 4, 5, 11). For example, spectra in Fig. 4 show that the HF bands disappear simultaneously with the increase in exposure temperature and are not observable for exposure temperatures greater than 400 K (Figs. 4c and 4d). It is also of interest to note that the removal or shift of the high-frequency band was invariably accompanied with the growth of low-frequency

bands, suggesting that the multicarbonyls are transformed progressively to the monocarbonyl form of bonded CO.

5. If the annealing behavior of various IR bands is compared, we observe that the surface species formed during CO + H_2 exposure are far less stable compared to those formed in the exposure of CO alone. For example, most of the CO bands in Fig. 2 were removed by pumping at room temperature, whereas the spectrum remained almost unchanged under identical conditions when the adsorbate was CO alone (Fig. 10a). Similarly, a comparison of Figs. 5 and 12 reveals that a lesser amount of CO remains accumulated over the catalyst surface in the CO + H_2 exposure at higher temperatures as well. Thus, the areas of broadband in the 2100–1900 cm^{-1} region were at least two times larger in Fig. 12 than the areas of corresponding bands in Fig. 5.

Relative intensities of various peaks as shown in Table 1 also indicate the presence of more prominent high-frequency bands, and hence of multicarbonyls, in the exposure of CO (Fig. 9) compared to the data observed for the CO + H_2 interaction (Fig. 2). The data in Fig. 10 further confirm that the exposure of hydrogen resulted in the removal of the 2137-cm^{-1} band and to the simultaneous buildup of lower-frequency bands due to the linearly bonded monocarbonyl form of CO.

It may thus be concluded that the coadsorbed hydrogen promoted transformation of multicarbonyl species to the linearly bonded monocarbonyl states as mentioned above.

6. The data in Fig. 4 show that the frequency of the 2050-cm^{-1} band shifted progressively to lower values with increasing CO + H_2 exposure temperature. A similar frequency shift was observed during prolonged exposure of a sample to CO + H_2 at an isothermal temperature of 470 K (Figs. 5a–5d). A similar temperature- and time-dependent frequency shift was also observed when a catalyst was exposed to carbon monoxide (Fig. 11). The frequency shift in ν_{CO} is a widely reported and reviewed phenomenon (*47, 49, 50*) which has been attributed to various factors, such as the influence of surface coverage on dipole–dipole coupling between chemisorbed species or the population of CO $2\pi^*$ orbitals due to metal–CO bonding, thus affecting the C–O bond order. The overall population of CO $2\pi^*$ orbitals may further depend on surface coverage due to a competition for the metal *d* electrons. The frequency shift shown in Figs. 4 and 11 is not related to the adsorbate pressure effect (*49*) since a constant pressure was maintained during experiments carried out in our study at different temperatures. The continuous decrease in the intensity of the 2050-cm^{-1} band may instead be attributed to decreasing availability of the sites responsible to these species. The fact that the ν_{CO} was not restored to original values on recooling confirms that some of the sites are progressively blocked, possibly due to carbon or hydrocarbon chains, resulting in the impeded growth of corresponding monocarbonyl species. Present data also indicate that the distinct metal sites are responsible for various CO binding states and some of these sites are more prone to poisoning.

7. As only Ru(CO) type species existed over the catalyst surface at temperatures above 400 K, when methane formation also begins (Fig. 8), it may be suggested that these species were direct precursors to methane.

8. The data in Fig. 2 show that out of all the bands, the bands at 2132, 2080–2070, and 1995 cm^{-1} were more stable and were observable after prolonged evacuation. As these bands are identifiable with the CO bonded with RuO_x, it appears that oxygen stabilizes CO bonding with Ru. A possible mechanism for such oxygen-induced CO stabilization is proposed by Yokomizo *et al.* (*16*).

Oxygenate Surface Complexes (1000- to 1700-cm^{-1} Region Bands)

We find no evidence of any oxygenated surface complexes (such as CHO_{ad} or

$HCHO_{ad}$) being formed as intermediates (*51*) in CO hydrogenation reactions in both the continuous flow and the static modes. The weak bands seen in the 1700–1000-cm^{-1} region (Fig. 1a) were also observed when a metal-free titania sample was exposed to CO_2 at room temperature (*37*). Also, no such bands were detectable in CO + H_2 exposures at higher temperatures (Figs. 1b–1d). The small concentration of oxygenated species seen in Fig. 1a may thus be considered a result of the CO_2 reaction which is found to be one of the reaction products (Fig. 8).

CONCLUSIONS

The main conclusions of our study can be summarized as follows

1. Different oxidation states of ruthenium serve as independent CO chemisorption sites, giving rise to distinct CO modes which may coexist simultaneously at a particular temperature.

2. The chemisorbed CO undergoes dynamic transformation from a multicarbonyl to a linearly bonded monocarbonyl form at a rate depending on the catalyst temperature.

3. The presence of H_2 does not affect the mode of CO binding on Ru but it promotes transformation of multicarbonyl to monocarbonyl species leading further to the formation of methylene groups at metal sites. Present data tend to suggest that the monocarbonyls are direct precursors to hydrocarbons.

4. Our data clearly show that the methylene group containing species formed in the CO + H_2 interaction are highly reactive to hydrogen when in the nascent state. Upon thermal treatment or after substantial growth, they may transform into inactive hydrocarbon species.

5. Present data also indicate that an optimum surface concentration of $-CH_2-$ groups or an optimum temperature is required for conversion of surface methylene groups to methane.

6. Various CO binding states arise due to distinct metal sites and the sites responsible for a particular M–CO (ν = 2050 cm^{-1}) species are selectively blocked on deposition of hydrocarbon chains at the catalyst surface.

7. It is suggested that the CO → hydrocarbon transformation may occur via more than one route, viz., direct transformation following a Bouduard process or via formation of a long chain of methylene groups. The contribution of these routes in overall product selectivity and in the reaction kinetics may depend on the metal and the experimental conditions such as the temperature, pressure, and hydrogen concentration, the details of which may not be speculated on at present.

ACKNOWLEDGMENTS

The authors thank Dr. V. B. Kartha, Head, Spectroscopy Division, BARC, for helpful discussions. We also thank the referees for critical comments and helpful suggestions.

REFERENCES

1. Bell, A. T., *in* "Proceedings, 9th International Congress on Catalysis" (M. J. Phillips and M. Ternan, Eds.), Vol. 5, p. 134. The Chemical Institute of Canada, Ottawa, 1988.
2. Anderson, R. B., "The Fischer Tropsch Synthesis." Academic Press, New York, 1984.
3. Vannice, M. A., *in* "Catalysis—Science and Technology" (J. R. Anderson and M. Boudart, Eds.), Vol. 3, p. 139. Springer-Verlag, Berlin, 1982.
4. Bell, A. T., *Catal. Rev. Sci. Eng.* **23,** 203 (1981).
5. Biloen, P., and Sachtler, W. M. H., *Adv. Catal.* **30,** 165 (1981).
6. Somorjai, G. A., *Catal. Rev. Sci. Eng.* **23,** 189 (1981).
7. Hoffman, F. M., and Robbins, J. L., *in* "Proceedings, 9th International Congress on Catalysis," Vol. 3, p. 1144, 1988.
8. Thampi, K. R., Kiwi, J., and Grätzel, M., *Nature* **327,** 506 (1987); also *in* "Proceedings, 9th International Congress on Catalysis (M. J. Phillips and M. Ternan, Eds.), Vol. 2, p. 837. The Chemical Institute of Canada, Ottawa, 1988.
9. Castner, D. G., Blackadar, R. L., and Somorjai, G. A., *J. Catal.* **66,** 257 (1980).
10. King, D. L., *J. Catal.* **51,** 386 (1978).
11. Dalla Betta, R. A., Piken, A. G., and Shelef, M., *J. Catal.* **35,** 54 (1974).
12. Taylor, K. C., Sinkevitch, R. M., and Klimisch, R. L., *J. Catal.* **35,** 34 (1974).
13. Robbins, J. L., *J. Catal.* **115,** 120 (1989).
14. Highfield, J. G., Ruterana, P., Thampi, K. R., and Grätzel, *in* "Structure and Reactivity of Surfaces

(C. Morterra, A. Zecchina, and G. Costa, Eds.), p. 469, Elsevier, Amsterdam, 1989.
15. Prairie, M. R., Renken, A., Highfield, J. G., Thampi, K. R., and Grätzel, M., *J. Catal.* **129,** 130 (1991).
16. Yokomizo, G. H., Louis, C., and Bell, A. T., *J. Catal.* **120,** 1 (1989).
17. Lynds, L., *Spectrochim. Acta* **20,** 1369 (1964).
18. Brown, M. F., and Gonzalez, R. D., *J. Phys. Chem.* **80,** 1731 (1976).
19. King, D. L., *J. Catal.* **61,** 77 (1980).
20. Davydov, A. A., and Bell, A. T., *J. Catal.* **49,** 332 (1977).
21. Chen, H.-W., Zhong, Z., and White, J. M., *J. Catal.* **90,** 119 (1984).
22. Solymosi, F., and Raskó, J., *J. Catal.* **49,** 240 (1977).
23. Kobayashi, M., and Shirasaki, T., *J. Catal.* **28,** 289 (1973).
24. Yamasaki, H., Kobori, Y., Noito, S., Onishi, T., and Tamaru, K., *J. Chem. Soc. Faraday Trans. I* **77,** 2913 (1981).
25. Zecchina, A., Guglielminotti, E., Bossi, A., and Camia, M., *J. Catal.* **74,** 225 (1982).
26. Guglielminotti, E., Zecchina, A., Bossi, A., and Camia, M., *J. Catal.* **74,** 240 (1982).
27. Guglielminotti, F., Zecchina, A., Bossi, A., and Camia, M., *J. Catal.* **74,** 252 (1982).
28. Kunznetsov, V. L., Bell, A. T., and Yermakov, Y. I., *J. Catal.* **65,** 374 (1980).
29. Ekerdt, J. G., and Bell, A. T., *J. Catal.* **58,** 170 (1979).
30. Solymosi, F., and Raskó, J., *J. Catal.* **115,** 107 (1989).
31. Unland, M. L., *J. Catal.* **31,** 459 (1973).
32. Dalla Betta, R. A., and Shelef, M., *J. Catal.* **48,** 111 (1977).
33. Dalla Betta, R. A., *J. Phys. Chem.* **79,** 2519 (1975).
34. Goodwin, J. G., Jr., Naccache, C., *J. Catal.* **64,** 482 (1980).
35. Thampi, K. R., Lucarelli, L., and Kiwi, J., *Langmuir* **7,** 2642 (1991).
36. Ruterna, P., Buffat, P-A., Thampi, K. R., and Grätzel, M., *Mater. Res. Soc. Symp. Proc.* **139,** 327 (1989).
37. Gupta, N. M., Thampi, K. R., Kamble, V. S., Öz, H., Gäumann, T., and Grätzel, M., unpublished results.
38. Gupta, N. M., Kamble, V. S., and Iyer, R. M., *in* "Proceedings 6th National Workshop on Catalysis, ISM, Dhanbad, Dec. 1991," to be published.
39. Solymosi, F., and Knözinger, H., *J. Catal.* **122,** 166, 1990.
40. Eischens, R. P., and Pliskin, W. A., "Advances in Catalysis" (A. Farkas, Ed.), Vol. 9, p. 662. Academic Press, New York, 1957.
41. Orita, H., Naito, S., and Tamaru, K., *J. Catal.* **112,** 176 (1988).
42. Araki, M., and Ponec, V., *J. Catal.* **44,** 439 (1976).
43. Wentrcek, P. R., Wood, B. J., and Wise, H., *J. Catal.* **43,** 363 (1976).
44. Gupta, N. M., Kamble, V. S., Annaji Rao, K., and Iyer, R. M., *J. Catal.* **60,** 57 (1979).
45. Pfnur, H., Menzel, D., Hoffmann, F., Ortega, A., and Bradshaw, A. M., *Surf. Sci.* **93,** 431 (1980).
46. Blyholder, G. J., *J. Phys. Chem.* **68,** 2772 (1964).
47. Primet, M., *J. Catal.* **88,** 273 (1984).
48. Vannice, M. A., Wang, S-Y., and Moon, S. H., *J. Catal.* **71,** 152 (1981).
49. Tanaka, K., and White, J. M., *J. Catal.* **79,** 81 (1983).
50. Peri, J. B., *in* "Catalysis—Science and Technology" (J. R. Anderson and M. Boudard, Eds.), Vol. 5, p. 171, Springer-Verlag, Berlin, 1984.
51. Vannice, M. A., *Catal. Rev. Sci. Eng.* **14**(2), 153 (1976).